Jurnal Teknologi

Abstract

The Reynold's Number Effect in High Swirling Flow in Unconfined Burner

Norwazan A. R.[a,b], Mohammad Nazri Mohd. Jaafar[b]

[a]*Faculty of Engineering, Universiti Pertahanan Nasional Malaysia, Kem Sg. Besi, 57000, Kuala Lumpur, Malaysia*
[b]*Department of Aeronautics & Automotive, Faculty of Mechanical Engineering, Universiti Teknologi Malaysia, 81310 UTM, Johor, Malaysia*

*Corresponding author: norwazan@upnm.edu.my

Article history

Received : 15 August 2014
Received in revised form :
15 October 2014
Accepted :15 November 2014

Graphical abstract

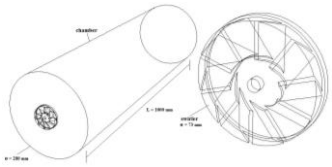

Abstract

The numerical simulations of swirling turbulent flows in isothermal condition in combustion chamber of burner were investigated. The aim is to characterize the main flow structures and turbulence in a combustor that is relevant to gas turbines. Isothermal flows with different inlet flow velocities were considered to demonstrate the effect of radial velocity. The inlet velocity, U_o is varied from 30 m/s to 60 m/s represent a high Reynolds number up to 3.00 X 10^5. The swirler was located at the upstream of combustor with the swirl number of 0.895. A numerical study of non-reacting flow in the burner region was performed using ANSYS *Fluent*. The Reynolds–Averaged Navier–Stokes (RANS) approach method was applied with the standard *k-ε* turbulence equations. The various velocity profiles were different after undergoing the different inlet velocity up to the burner exit. The results of velocity profile showed that the high U_0 give better swirling flow patterns.

Keywords: Simulation; swirling flow; Reynold's number; standard *k-ε*; inlet velocity U_0

1.0 INTRODUCTION

Swirlers are used as flame holders to control the mixture speed depending on the flame speed [1]. In addition, generating a swirling flow inside burners enhances the mixing of the different constituents of the mixture permitting, thus, a better control of the combustion process in terms of flame quality and pollutants emission.

Turbulent swirling flow in the combustor plays an important role in controlling the combustion processes and performances. Swirling flows have been investigated extensively that used in all kinds of practical combustion systems including gas turbine combustor of aero-engine and industrial, swirl burner, furnaces, cyclone combustor and others [2, 3]. Consequently, the flame structure and stability in combustion is extremely depends on the aerodynamics and mixing characteristics of fuel and oxidizer in their mixing region [3-6]. A swirling flow is cause of an impartation of a tangential component by usage of swirler positioned within the burner [5, 7]. The appropriate of swirl produces a large adverse pressure gradient in the direction of flow, which promotes the reverse flows. Thus, the formation of a flow pattern provides an aerodynamic blockage and reduced velocities necessary to stabilize the flame [4-5].

The prediction of the swirling flow characteristics in the combustor can be done using numerical simulation in order to optimize the design. A numerical study of the application computational fluid dynamics (CFD) is a great potential in order to investigate isothermal and combustion process. Turbulence models that are great practical importance are three-dimensional and time-dependent. Computational methods of solving the differential equations of fluid dynamics are well advanced [8]. Turbulent behaviour of inertial systems at every time in the space continuum seems to appear similar characteristics such as vortex structures and structural inhomogeneity [9]. Turbulent is the state of fluid processing a non-regular or irregular motion such that velocity at any point may vary both in magnitude and direction with time. Turbulent motion is accompanied by the formulation of eddies and the rapid interchange of momentum in the fluid. Turbulence sets up greater stresses throughout the fluid and causes more irreversibility and losses. Turbulence is characterized by high levels of momentum, heat and mass transport due to turbulent diffusivity in flow.

Palm *et.al* [10] were studied experimentally the effect of Reynold's number to the flow in annular channel. The results of axial and tangential velocity are normalized using the bulk axial velocity that is relatively insensitive to the inner jet flow velocity.

The maximum velocities for both are formed by high Re. Mathur and Maccallum [11] were studied about various angle of axial swirler. The flows showed that axial swirler of 60° vane angles has greater central recirculation vortex not only extended upstream to the hub of swirler but slightly blocked the annular flow area at the exit swirler. Thus, the axial swirler of 45° vane angle showed central recirculation zone was firmly established.

A recirculation zone is created downstream of the swirler in the center of flow. This is will effects primarily promoting fuel and air mixing and assisting the control of combustion temperature in the combustion zone. Therefore, the mixture provides the ignition energy for the fuel to ignite and stabilize the flame [12]. In non-premixed condition, fuel is injected in shear region formed near to the zero streamline boundary and recirculation region which provides the low velocity region for flame stabilization with the evolution of high temperatures from the flame. For flames operating in diffusion mode, the reaction zone is stabilized to result in large temperature gradients and hot-spot regions in the entire combustion chamber that result in high NO_x levels from the combustion of fuels [13].

The swirl intensity is generally characterized by the swirl number, defined as the ratio of the axial flux of azimuthal momentum to the axial flux of axial momentum [4, 7, 12, 14-17]. The swirl number is a measure of the strength of the swirling flow [18]. The swirl number is defined as:

$$S = \frac{G_\theta}{G_x R} \tag{3}$$

where,

$$G_\theta = \int_0^\infty r^2 \rho(u_a u_t + \overline{u'_a u'_t})\, dr \tag{4}$$

and

$$G_x = \int_0^\infty r(\rho(u_a^2 + \overline{u'_a u'_a}) + (p - p_{ref}))dr \tag{5}$$

where U,W and ρ are the axial velocity, tangential velocity and density respectively. For axial vane axial swirler, the swirl number is related to the swirl angle, θ, inner r_i and outer radius r_0 as given by [19, 20];

$$S = \frac{\int_0^{R_0} \rho u_a u_t r^2 dr}{R \int_0^{R_0} \rho u_a^2 r dr} \tag{6}$$

Steady-state, incompressible, turbulent flows are governed by the Reynolds-averaged continuity and Navier-Stokes equations. The conservation form of these equations can be written as

Continuity:

$$\frac{\partial U}{\partial z} + \frac{1}{r}\frac{\partial}{\partial r}(rV) = 84 \tag{7}$$

Axial Momentum:

$$U\frac{\partial U}{\partial z} + V\frac{\partial U}{\partial r} = -\frac{1}{\rho}\frac{\partial P}{\partial z} + v\left(\frac{\partial^2 U}{\partial z^2} + \frac{1}{r}\left(r\frac{\partial U}{\partial r}\right)\right) - \frac{\partial}{\partial z}\langle u^2\rangle - \frac{\partial}{\partial r}\langle uv\rangle - \frac{\langle uv\rangle}{r} \tag{8}$$

Standard k-ε model the turbulent viscosity is computed by the combination of the turbulence kinetic energy, k and its dissipation rate, ε as follows

$$\mu_t = \rho C\mu \frac{k^2}{\varepsilon} \tag{9}$$

The two differential equations are used to describe the turbulence kinetic energy, k and dissipation rate of turbulence, ε in Equations (10) and (11), respectively [2, 8, 12, 21, 22];

$$\rho\frac{Dk}{Dt} = \frac{\partial}{\partial x_i}\left[\left(\mu + \frac{\mu_t}{\sigma_k}\right)\frac{\partial k}{\partial x_j}\right] + P - \rho\varepsilon \tag{10}$$

and

$$\rho\frac{D\varepsilon}{Dt} = \frac{\partial}{\partial x_j}\left[\left(\mu + \frac{\mu_t}{\sigma_\varepsilon}\right)\frac{\partial k}{\partial x_i}\right] + C_{1\varepsilon}\frac{\varepsilon}{k}P - C_{2\varepsilon}\rho\frac{\varepsilon^2}{k} \tag{11}$$

(11)

P represents the production of turbulence kinetic energy. The σ_k, σ_ε, $C_{1\varepsilon}$, $C_{2\varepsilon}$ and C_μ are model constants.

In the present study, the numerical simulation of swirling flow, issuing from the annular inlet of a burner, using different turbulence models is considered. The Reynolds-Averaged Navier Stokes (RANS) standard k-ε turbulence models, implemented in the commercial software FLUENT 14.0, were used. A 3D computational grid of 1.5 million cells was employed for the standard k-ε simulation. This comparative study is using a high swirl numbers of 0.895 was conducted. The experimental and numerical approaches are, first, presented in the next section, followed by results of the effects of inlet air velocity are discussed.

2.0 METHODOLOGY

The Computer Aided Design (CAD) modeling was created using *AutoCAD 2012* software in three-dimensional (3D) according to the actual laboratory scale of liquid fuel burner. The 3D CAD modeling was assembled and exported to produce meshing and set-up the boundary conditions. The meshing was composed primarily of tetrahedral mesh elements including hexahedral, pyramidal and wedge with various sizes. In the front of combustor burner, the inlet and swirler were located with the element mesh were built in fine grids. 3D Reynolds-Averaged Navier Stokes (RANS) computations modeling of the entire section including swirl generation system and burner have been performed using commercial CFD-software ANSYS *Fluent*. The actual dimension of entire combustor burner is represented in Figure 1. The liquid fuel burner was built in 280 mm of diameter and 1000 mm of length. The axial swirler and fuel nozzle are centered in the middle of burner shows the axial swirler in 50 degree of vanes angle with the swirl number, S = 0.895. The nozzle's diameter of fuel inlet is 8 mm and swirler of air inlet is approximately 73 mm.

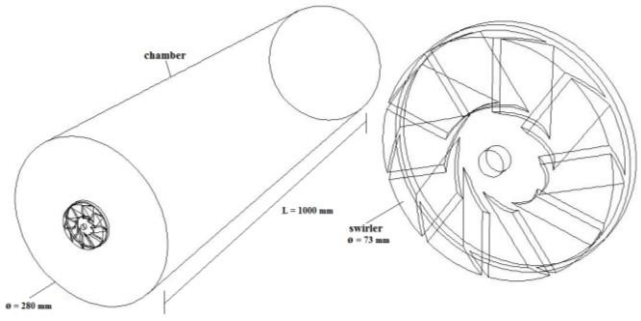

Figure 1 The model of overall liquid fuel burner

This numerical study, simulations were performed to evaluate the radial velocity and tangential velocity of swirling flow in isothermal condition. The initial velocity was assigned at the inlet entering the swirler in the range of 30 m/s to 60 m/s. These velocities represented the Reynolds number for each case. In this numerical simulation, the air was chosen as a working fluid with the density, ρ = 1.225 kg/m^3 and kinematic viscosity, ν =1.771 X 10^{-5} kg/m-s. The convergence of this solution for each conservation equation was reduced to about 10^{-5}.

The transverse flow field data were measured at different location of burner length at *z*-planes. There were 5 *z*-planes have been studied up to x = 140 mm in axial direction which represented as x/D ratio as x/D = 0.1, x/D = 0.2, x/D = 0.3, x/D = 0.4 and x/D = 0.5.

3.0 RESULTS AND DISCUSSION

The velocity magnitude along the combustor was measured using experimental and numerical method. Figure 2 shows good agreement results between both methods in axial direction along the combustion chamber of burner. The experiment data is measured in axial distance at 10 different locations at the center core of flow. This comparison data was investigated by using the same parameter such as the same input velocity at 30 m/s and 50 degree of swirl vane angles. They showed that the numerical simulation result has similar trend of velocity magnitude with the experimental data.

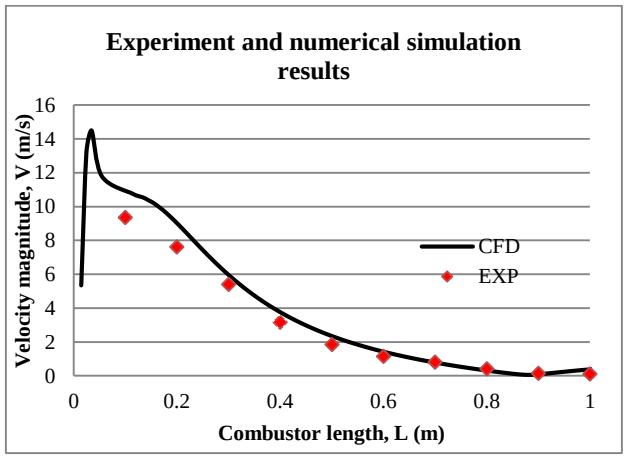

Figure 2 Velocity magnitude profile along combustor

Swirling jet flow is the results of impartation of axial velocity produced by swirl generator. The large reverse flow zone that induced by the vanes of swirler in axial direction is identified by negative axial velocity in isothermal condition known as center recirculation zone. There are also other recirculation zones at the corner of the chamber namely corner recirculation zone. Comparison of the flow patterns for the swirl number of 0.895 shows similarity in three velocities types that are varied in different U_0. These results presented the axial and tangential velocity in radial distance where it shows the strength of swirl flow that influenced by axial, radial and tangential velocities components [23].

Figure 3 shows the reverse flow velocity distribution contour, termed as central recirculation zone in the mid plane in each case of U_0 of 30 m/s, 40 m/s, 50 m/s and 60 m/s respectively. The flow downstream of 50˚ swirler with the highest U_o has a maximum reverse velocity of 19.56 m/s. Thus, the maximum reverse velocity magnitudes of 30 m/s, 40 m/s and 50 m/s of U_o were found as 12.34 m/s 13.71 m/s and 16.88 m/s respectively. These contours were displayed by plotting the negative axial velocities in the range of 0 to maximum negative axial velocity flow within the entire recirculation zone. As seen in Figure 4, the recirculation zone of 60 m/s of U_o is more width (is wider) and longer. It shows that the central recirculation zone has a largest width and longest length by increasing the U_o. As reported by Raj [24], the effect of various axial swirler on square chamber also illustrated that the length and width of recirculation zone increased with increase in the vane angle.

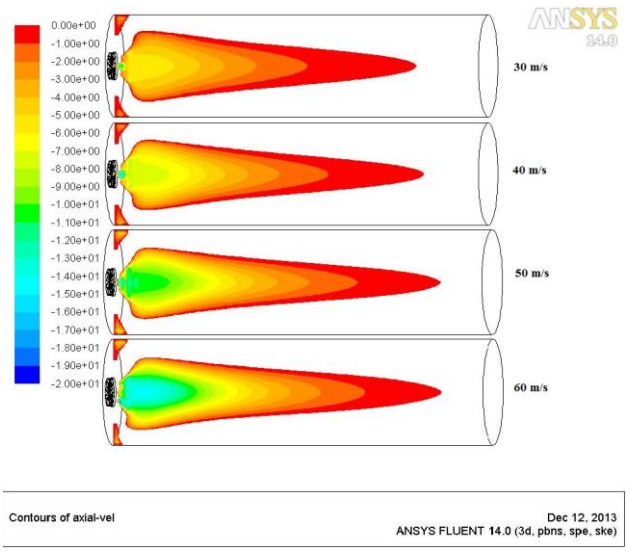

Figure 3 The contour of axial velocity flow

Axial Velocity Profiles

The importance of axial velocity profiles was illustrated by jet boundary, degree of expansion and region of high velocity gradient [15]. It is also defined by the boundaries of the forward- and reverse-flow zones. Generally, the zone behind swirler placed in strong axial stream and their formation of a downstream known as recirculation zone [25] depends on the S_N and Reynold's number. Steady state calculations were carried out for flows of different inlet velocities entering the swirler. The inlet velocity, U_0 represented as a Reynold's Number, Re different in each cases by setting the proportion of the air entering the chamber through the swirler. The effect of the U_0 was investigated by comparing the flow field behind the swirler for 5 normalized planes; x/D included axial, radial and tangential velocities.

The graphs were presented as a half of radial distance that is slightly symmetry for positive and negative values. The axial velocity presents in the simulation of the entire combustion chamber. But the result presents was plotted till transverse plane x/D=0.5, which corresponds to maximum of velocity in each cases while the rest is similar. The axial velocity peaks are changed at r/D = 0.2 for all U_0 cases. The highest axial velocity

affected by the U_0 = 60 m/s. it also observed that this case shows has a highest reverse velocity at the center core of flow zones from 0 to 0.1 of r/D. The case of highest U_0 also represents the highest reverse velocity. Thus, the lowest U_0 has the lowest reverse velocity that occurred at the center of flow after entering the swirler. It shows that by increasing the U_0, the axial velocity becomes higher respectively at initial state nearly after entering the swirler. Then, the axial velocity has changes slowly towards downstream flow. These changes of axial velocity are shown differently in x/D = 0.2 till x/D = 0.5 planes. As seen in Figure 4, the lowest U_0 is varying the axial velocity slowly compared to the highest U_0. The highest U_0 of 60m/s has large differences of axial velocity from beginning to the end of the flow.

After x/D = 0.5, the axial velocity graphs had no drastic changes and not significantly to present. At x/D = 0.5, it shows that the axial velocity for all cases becomes similar and started to be flattened at the center core in this radial distance. It is observed that the highest U_0 gives a good improvement on swirling flow. Thus, it could provide the good mixing for fuel and air for flame stabilization in the combustion process.

Radial Velocity Profiles

In case of radial velocity effects in Figure 5, the same parameters of each cases of U_0 were shown. In x/D = 0.1 of transverse plane, the highest U_0 has minimum radial velocity as compared to the lowest U_0. Concurrently, the radial flow patterns were similar for each case. As low as U_0, the radial velocity becomes higher. The higher peaks of radial velocity are located at radial distance, r/D = 0.2. These radial velocities of flows are decreasing near to the wall of chamber. When the flow was forwarded to the downstream, the radial velocity becomes flatten at the center core zones and had a highest peak near to the wall. These radial velocity diminished as flow expands along the wall at x/D = 0.2. Then, the radial velocity were started to decrease to x/D = 0.3 for all cases of U_0. Gradually, these flow decreasing towards downstream and similar in each cases of U_0. Observation from Zhuowei [26], it is found that the tangential velocity value exhibits the forced-vortex characterized by increased the tangential velocity in central region while the free-vortex characterized by decreased the tangential velocity when approaching the wall. The similar finding in these results, the tangential velocity presented that is increasing and moves forward to the walls in high U_0.

Tangential Velocity Profiles

As shown in Figure 6, the tangential velocity exhibits similar behaviour in each case from initial state. In x/D = 0.1, the trend of tangential velocities are slightly similar. The tangential velocity peaks is highest with the lowest value of U_0 at r/D = 0.2. In contrast, the highest U_0 is produced with the lowest tangential velocity. Then, when the flow moves towards downstream, the tangential velocities are becomes the same. Not much differences for each case of U_0. All the velocities diminish as the flow expands along the wall to the end towards the chamber outlet. As expected, the tangential velocity had maximum differences only at initial state of entering chamber (x/D = 0.1 plane) near the swirler. Then, as expands along radial distance after x/D = 0.1 plane, these tangential velocities behaves similarly.

4.0 CONCLUSION

The eddy-dissipation model and standard *k-ε* turbulence approach method were used in this study to evaluate the axial swirler adopted inside an unconfined burner are well compared. The simulation was defined by axial, radial and tangential velocity with the various U_0 entering the swirling flow. This study was also investigated to determine a better center recirculation zone in order to get better mixing with a suitable vane angle of axial swirler using standard *k-ε* turbulence model are still practical and reasonable. The 3D flow behaviour was found behind the swirler for all three velocities, which decayed far away downstream. It is found that the graphs of axial velocity, radial velocity and tangential velocity have obvious differences at the early in upstream that strongly dependent on the proportion of flow entering axial swirler that given a larger effected by high U_0. In the early state, after x/D = 0.1 plane, there are three velocities show the graph patterns had starting changes in similar pattern for all differences of U_0. It can be concluded that with a high U_0 is produced a better mixing and good swirling flow with attached in unconfined burner.

Acknowledgements

The authors would like to thankful to Ministry of Science, Technology and Innovation (MOSTI) for their funding under Sciencefund Grant 4S046 as well as UTM for their supports.

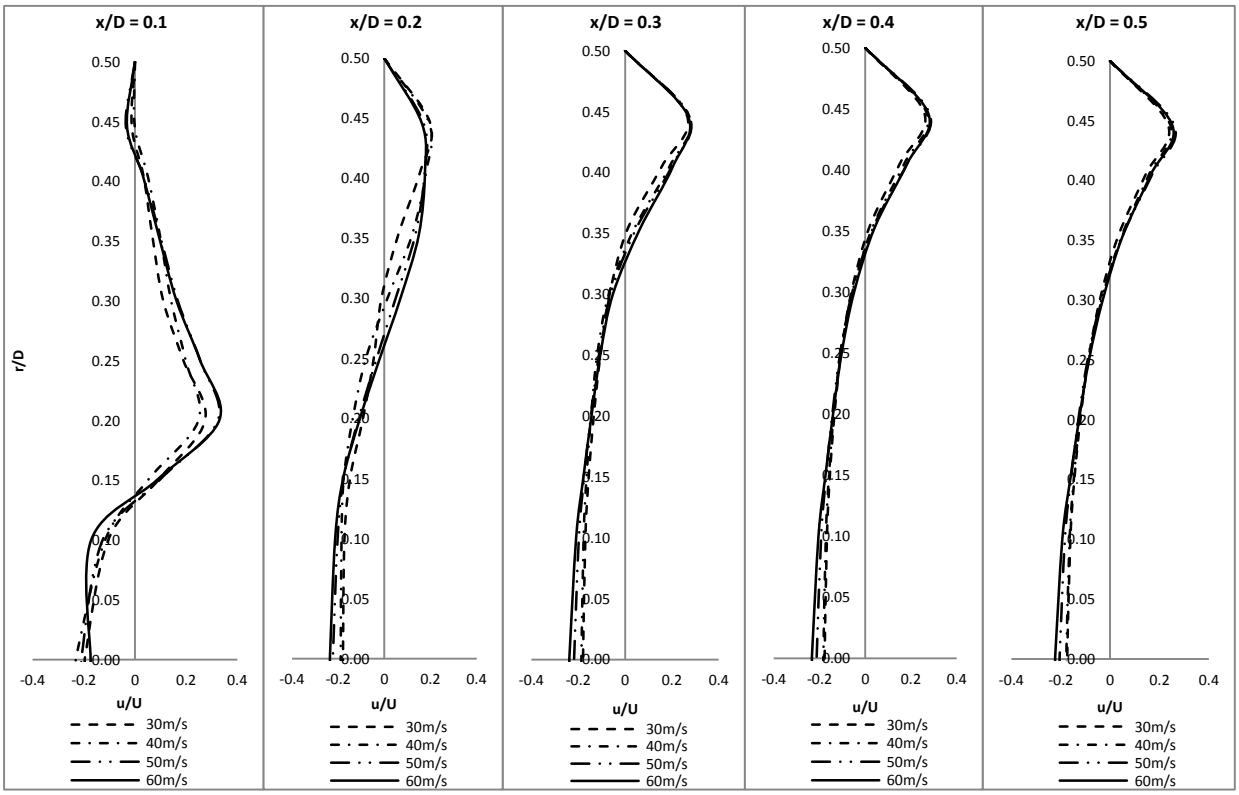

Figure 4 Normalized axial velocity profiles

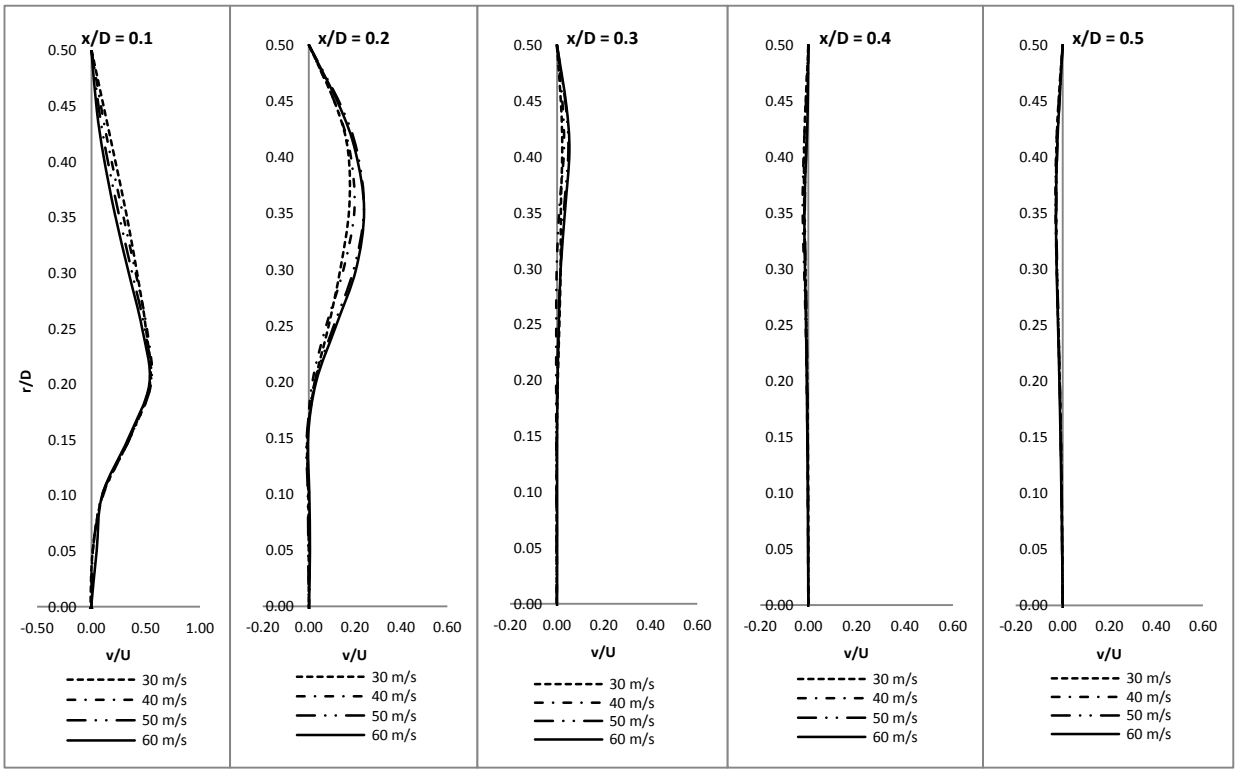

Figure 5 Normalized radial velocity profiles

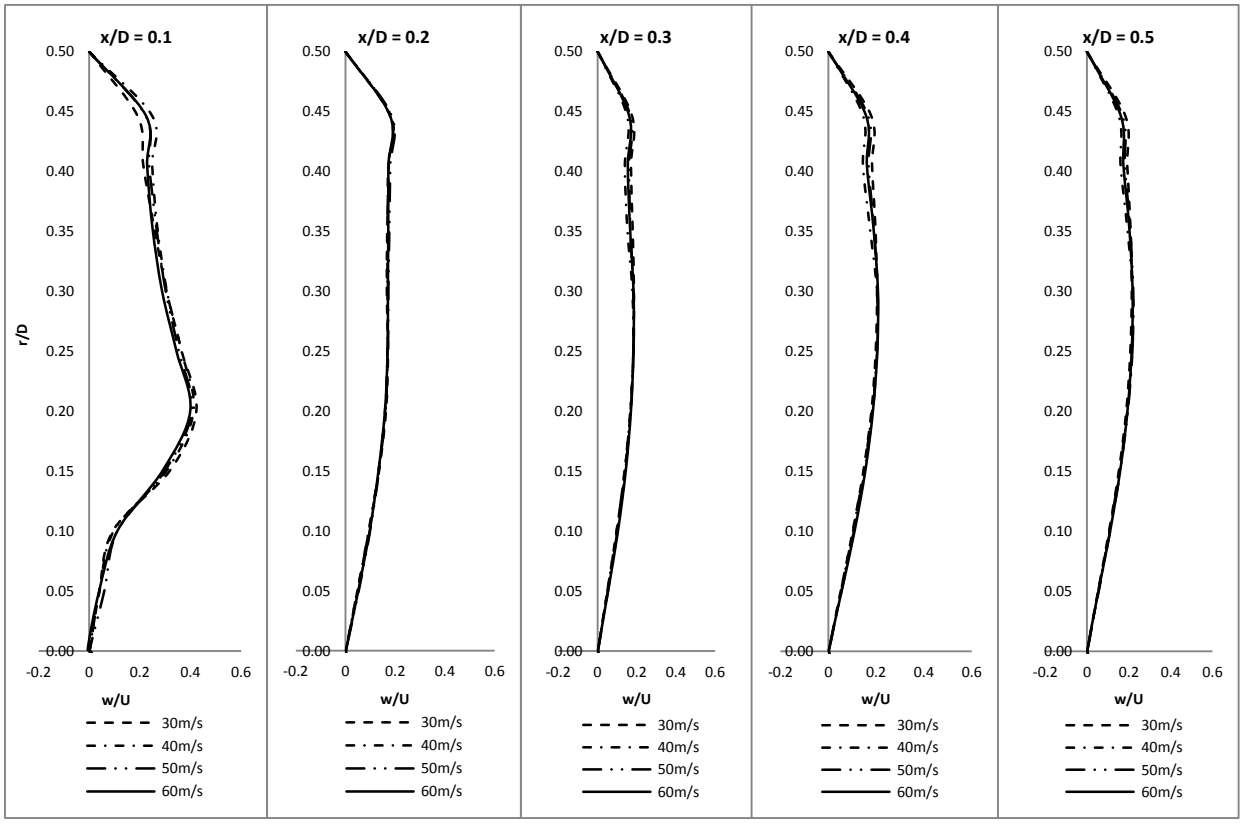

Figure 6 Normalized tangential velocity profiles

References

[1] Mohd Jaafar, M. N., Jusoff, K., Osman, M. S., and Ishak, M. S. A. 2011. Combustor Aerodynamics Using Radial Swirler, *International Journal of Physics Sciences*. 6(13): 3091–3098.

[2] Ridluan, A., Eiamsa-ard, S., and Promvonge, P. 2007. Numerical Simulation of 3D Turbulent Isothermal Flow in a Vortex Combustor. *International Communication in Heat and Mass Transfer*. 34: 860–869.

[3] Litvinov, I. V., Shtork, S. I., Kuibin, P. A., Alekseenko, S. V., and Hanjalic, K. 2013. Experimental Study and Analytical Reconstruction of Processing Vortex in a Tangential Swirler. *International Journal of Heat and Fluid Flow*. 42: 251–264.

[4] Syred, N., and Beer, J. M. 1974. Combustion in Swirling Flows: A Review. *Combustion and Flame*. 23: 143–201.

[5] Sloan, D. G., Smith, P. J., and Smoot, L. D. 1986. Modeling of Swirl in Turbulent Flow Systems. *Prog. Energy Combustion Science*. 12: 163–250.

[6] Eldrainy, Y. A., Mohd Jaafar, M. N., and Mat Lazim, T. 2008. Numerical Investigation of the Flow Inside Primary Zone of Tubular Combustor Model. *Jurnal Mekanikal*. 26: 162–176.

[7] Yegian, D. T., and Cheng, R. K. 1998. Development of a Vane-swirler for Use in a Low No_x Weak-Swirl Burner. *Combust. Sci. Technol.* 139(1–6): 207–227.

[8] Launder, B. E., and Spalding, D. B. 1974. The Numerical Computation of Turbulent Flows. *Computer Methods in Applied Mechanics and Engineering*. 3: 269–289.

[9] Magnussen, B.,F., and Hjertager, B. H. 1976. On Mathematical Modeling of Turbulent Combustion with Special Emphasis on Soot Formation and Combustion. *16th Symposium (International) on Combustion, Combustion Institute*. 719–729.

[10] Palm, R., Grundmann, S., Weismuller, M., Saric, S., Jakirlic, S., and Tropea, C. Experimental Characteristization and Modeling of Inflow Conditions for a Gas Turbine Swirl Combustor.

[11] Mathur, M. L. and MacCallum, N. R. L. 1967. Swirling Air Jets Issuing from Vane Swirlers. Part 1: Free Jets. *Journal of the Institute of Fuel*. 40: 214–225.

[12] Eldrainy, Y. A., Saqr, K. M. Aly, H. S., and Mohd Jaafar, M. N. 2009. CFD Insight of the Flow Dynamics in a Novel Swirler for Gas Turbine Combustors. *International Communications in Heat and Mass Transfer*. 36: 936–941.

[13] Khalil, A. E. E. and Gupta, A. K. 2011. Distributed Swirl Combustion for Gas Turbine Application. *Applied Energy*. 88: 4898–4907.

[14] Orbay, R. C., Nogenmyr, K. J., Klingmann, J., and Bai, X. S. 2013. Swirling Turbulent Flows in a Combustion Chamber with and Without Heat Release. *Fuel*. 104: 133–146.

[15] Pollard, A., Ozem, H. L. M., and Grandmaison, E. W. 2005. Turbulent, Swirling Flow Over an Asymmetric Constant Radius Surface. *Experimental Thermal and Fluid Science*. 29: 493–509.

[16] Beltagui, S. A., Kenbar, A. M. A., and Maccallum, N. R. L. 1993. Comparison of Measured Isothermal and Combusting Confined Swirling Flows: Peripheral Fuel Injection. *Experimental Thermal and Fluid Science 1993*. 6: 147–156.

[17] Bourgouin, J. F., Moeck, J., Durox, D., Schuller, T., and Candel, S. 2013. Sensitivity of Swirling Flows to Small Changes in the Swirler Geometry. *C. R. Mecanique*. 341: 211–219.

[18] Murphy, S., Delfos, R., Pourquie, M. J. B. M., Olujic, Z., Jansens, P. J., and Nieuwstadt, F. T. M. 2007. Prediction of Strongly Swirling Flow Within an Axial Hydrocyclone Using Two Commercial CFD Codes. *Chemical Engineering Science*. 62: 1619–1635.

[19] Beer, J. M. and Chigier, N. A. 1972. *Combustion Aerodynamics*. Applied Science Publishers Ltd.

[20] Lilley, D. G., Prediction of Inert Turbulent Swirl Flows. *AIAA Journal*. 11(7): 955–960.

[21] Datta, A., and Som, S. K. 1999. Combustion and Emission Characteristics in a Gas Turbine Combustor at Different Pressure and Swirl Conditions. *Applied Thermal Engineering*. 19: 949–967.

[22] Xia, J. L., Yadigaroglu, G., Liu, Y. S., Schmidli, J., and Smith, B. L. 1998. Numerical and Experimental Study of Swirling Flow in a Model.

Int. Journal Heat Mass Transfer. 41(11): 1485–1497.
[23] Syred, N., Abdulsada, M., Griffiths, A., Doherty, T.O., and Bowen, 2012. The Effect of Hydrogen Containing Fuel Blends Upon Flashback in Swirl Burners. *Applied Energy*. 89: 106–110.
[24] Raj, R. T. K., and Ganesan, V. 2008. Study On The Effect Of Various Parameters on Flow Development Behind Vane Swirlers. *International Journal of Thermal Sciences*. 47: 1204–1225.
[25] Al-Abdeli, Y. M., and Masri, A. R. 2003. Recirculation and Flowfield Regimes of Unconfined Non-Reacting Swirling Flows. *Experimental Thermal and Fluid Science*. 27: 655–665.
[26] Zhuowei, L., Kharoua, N., Redjem, H., and Khezzar, L. 2012. RANS and LES Simulation of a Swirling Flow in a Combustion Chamber with Different Swirl Intensities. *Proceeding of CHT-12, ICHMT International Symposium on Advances in Computational Heat Transfer*.